Inflammasome activation leads to Caspase-1–dependent mitochondrial damage and block of mitophagy

Jiujiu Yu[a,1], Hajime Nagasu[a,1], Tomohiko Murakami[a,2], Hai Hoang[a], Lori Broderick[b,c], Hal M. Hoffman[b,c], and Tiffany Horng[a,3]

[a]Department of Genetics & Complex Diseases, Harvard School of Public Health, Boston, MA 02115; [b]Department of Pediatrics, University of California, San Diego, La Jolla, CA 92093; and [c]Rady Children's Hospital, San Diego, CA 92123

Edited by Ruslan Medzhitov, Yale University School of Medicine, New Haven, CT, and approved September 22, 2014 (received for review August 4, 2014)

Inflammasomes are intracellular sensors that couple detection of pathogens and cellular stress to activation of Caspase-1, and consequent IL-1β and IL-18 maturation and pyroptotic cell death. Here, we show that the absent in melanoma 2 (AIM2) and nucleotide-binding oligomerization domain-like receptor pyrin domain-containing protein 3 (NLRP3) inflammasomes trigger Caspase-1–dependent mitochondrial damage. Caspase-1 activates multiple pathways to precipitate mitochondrial disassembly, resulting in mitochondrial reactive oxygen species (ROS) production, dissipation of mitochondrial membrane potential, mitochondrial permeabilization, and fragmentation of the mitochondrial network. Moreover, Caspase-1 inhibits mitophagy to amplify mitochondrial damage, mediated in part by cleavage of the key mitophagy regulator Parkin. In the absence of Parkin activity, increased mitochondrial damage augments pyroptosis, as indicated by enhanced plasma membrane permeabilization and release of danger-associated molecular patterns (DAMPs). Therefore, like other initiator caspases, Caspase-1 activation by inflammasomes results in mitochondrial damage.

inflammasomes | mitochondrial damage | pyroptosis | mitophagy

Inflammasomes are cytosolic complexes that mediate Caspase-1 activation in response to pathogen infection and cellular stress (1, 2). They consist of a regulatory subunit, which couples stimulus recognition to complex assembly; Caspase-1, the effector subunit; and the adaptor protein Asc. The best-characterized inflammasomes include the AIM2 inflammasome, which detects cytosolic DNA during bacterial and viral infection, and the NLRP3 inflammasome, which is activated by many stimuli in a variety of settings including infection and metabolic inflammation. Although not entirely clear, one plausible model of NLRP3 inflammasome activation is the generation of some mitochondria-associated signal by mitochondrial destabilization (3, 4). Recruitment of Caspase-1 into the inflammasome complex leads to its activation, autoprocessing, and subsequent substrate cleavage.

The prototypical inflammasome-mediated functions are IL-1β and IL-18 maturation and induction of pyroptosis (1). Additionally, inflammasomes control other processes like unconventional secretion of intracellular proteins (5), such as DAMPs like high mobility group box 1 (HMGB1) (6), and regulation of autophagy (7, 8). These examples suggest the existence of additional inflammasome effector activities that are likely to vary in a context-dependent manner. Interestingly, a recent report indicated that activation of the NLRP3 inflammasome by extracellular ATP leads to NLRP3-dependent dissipation of the mitochondrial membrane potential (9), but subsequent studies proposed that such mitochondrial damage is solely a trigger of inflammasome activation (10, 11) because it occurs normally in the absence of the NLRP3 inflammasome (11). Thus, the relationship between NLRP3 inflammasome activation and mitochondrial damage remains unclear.

Pyroptosis is a Caspase-1–mediated, proinflammatory form of cell death. It occurs during infection by many intracellular pathogens where it can critically eliminate an intracellular replication niche (12), as well as other settings (13, 14), but experimental demonstration of its physiological role is hampered by the lack of mechanistic insights into its regulation. Pyroptosis shares some features with necrosis (such as loss of plasma-membrane integrity and release of intracellular contents) and others with apoptosis (including DNA fragmentation and nuclear condensation) (12). Mitochondrial damage critically underlies apoptosis mediated by initiator caspases like Caspase-8 and Caspase-9. Upon activation by death receptors, Caspase-8 cleavage of the protein Bid precipitates mitochondrial outer membrane permeabilization (MOMP), resulting in dissipation of the membrane potential, disruption of mitochondrial function, and release of apoptosis-promoting factors from the intermembrane space (15). MOMP can also lead to mitochondrial permeability transition (MPT), or breach of integrity of the inner membrane caused by opening of an inner membrane pore, which further amplifies mitochondrial damage (16). Whether mitochondrial damage contributes to pyroptosis and in general how pyroptosis is regulated, including the relevant substrates, are not clear.

Results

Amplification of Mitochondrial Damage by the NLRP3 Inflammasome. Recent studies suggest that mitochondrial damage may or may not be triggered by the NLRP3 inflammasome (9, 11). Here, we decided to reexamine this issue using additional stimuli, extended time courses, and several readouts of mitochondrial damage.

Significance

Sensors of the innate immune system trigger the induction of inflammatory responses upon infection and cellular stress. One such sensor is the inflammasome pathway, which is best described for its role in the production of the inflammatory cytokines IL-1β and IL-18. Other effector functions of the inflammasome pathway remain less well defined, and here we show that activation of this pathway leads to induction of mitochondrial damage and dismantling of the organelle. We link such mitochondrial damage to another inflammasome-regulated process called pyroptosis, which is a proinflammatory form of cell death. In summary, we characterize the role of mitochondrial damage during activation of the inflammasome pathway, of relevance to host defense and other physiological and pathophysiological settings.

Author contributions: T.H. designed research; J.Y., H.N., T.M., H.H., and L.B. performed research; H.M.H. contributed new reagents/analytic tools; J.Y., H.N., T.M., L.B., H.M.H., and T.H. analyzed data; and T.H. wrote the paper.

The authors declare no conflict of interest.

This article is a PNAS Direct Submission.

[1]J.Y. and H.N. contributed equally to this work.

[2]Present address: Department of Molecular and Cellular Biochemistry, Osaka University Graduate School of Dentistry, 1-8 Yamada-Oka, Suita, Osaka 565-0871, Japan.

[3]To whom correspondence should be addressed. Email: thorng@hsph.harvard.edu.

This article contains supporting information online at www.pnas.org/lookup/suppl/doi:10.1073/pnas.1414859111/-/DCSupplemental.

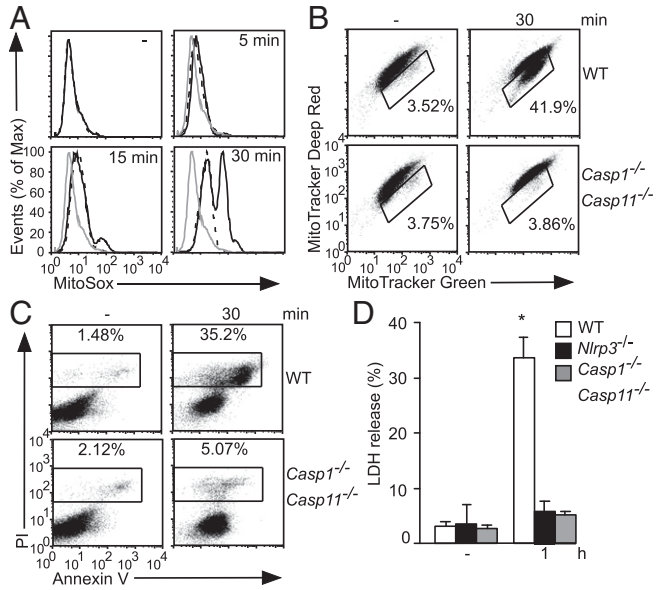

Fig. 1. The NLRP3 inflammasome amplifies mitochondrial damage. LPS-primed BMDMs of the indicated genotypes were stimulated with ATP, followed by staining with MitoSox (gray line, WT unstimulated; black line, WT; dashed line, Casp1$^{-/-}$Casp11$^{-/-}$) (*A*), Mitotracker Green and Mitotracker Deep Red (*B*), or AV/PI (*C*), or analysis in LDH release assay (*D*). In *B*, gated cells stain less brightly with Mitotracker Deep Red (i.e., downward shift), indicative of loss of $\Delta\Psi_m$. In *D*, * indicates $P < 0.05$ relative to *Casp1*$^{-/-}$*Casp11*$^{-/-}$ and *Nlrp3*$^{-/-}$ BMDMs ($n \geq 3$).

Consistent with previous reports, ATP treatment of lipopolysaccharide (LPS)-primed bone marrow-derived macrophages (BMDMs) triggered rapid changes to mitocondrial ROS (mROS) production and membrane potential ($\Delta\Psi_m$). Importantly, such changes were largely but incompletely dependent on the NLRP3 inflammasome. ATP triggered an initial increase in mROS production that is evident in the time-dependent increases in MitoSox staining in WT, *Nlrp3*$^{-/-}$, and *Casp1*$^{-/-}$*Casp11*$^{-/-}$ BMDMs whereas, at later time points, further increases are detectable in a subset of WT but not *Nlrp3*$^{-/-}$ and *Casp1*$^{-/-}$*Casp11*$^{-/-}$ BMDMs (Fig. 1*A* and Fig. S1*A*). Thus, ATP stimulation directly increased mROS production followed by NLRP3 inflammasome-mediated amplification of this response. Another indication of mitochondrial damage is dissipation of $\Delta\Psi_m$, which we examined by costaining with Mitotracker Green and Deep Red, dyes that are taken up in a $\Delta\Psi_m$-independent and -dependent manner, respectively. In response to ATP treatment, an initial mitochondrial membrane hyperpolarization is followed by depolarization (i.e., increase and decrease in Mitotracker Deep Red staining, respectively) (Fig. 1*B*). Membrane hyperpolarization occurred independently of the NLRP3 inflammasome (i.e., seen in all genotypes), but subsequent depolarization was strictly inflammasome-dependent (i.e., seen only in a subpopulation of WT cells) (Fig. 1*B* and Fig. S1*A*). Use of TMRM, a $\Delta\Psi_m$-sensitive dye, also indicated Caspase-1–dependent depolarization during ATP stimulation (Fig. S1*B*). ATP treatment in the absence of LPS priming, which is insufficient to activate the NLRP3 inflammasome, triggered modest increases in mROS production and mitochondrial hyperpolarization without depolarization (Fig. S1*C*), similar to the mitochondrial damage profile of *Casp1*$^{-/-}$*Casp11*$^{-/-}$ BMDMs stimulated with LPS plus ATP (Fig. 1 *A* and *B*). As expected, ATP-mediated activation of the NLRP3 inflammasome induced pyroptotic cell death as indicated by Annexin V (AV)/propidium iodide (PI) staining and lactate dehydrogenase (LDH) release (Fig. 1 *C* and *D*).

Stimulation of BMDMs with nigericin, another activator of the NLRP3 inflammasome, also induced inflammasome-dependent mitochondrial damage, as indicated by Caspase-1–dependent depolarization and mROS induction (Fig. S1 *D*–*F*). Of note, ATP and nigericin treatment seemed to directly perturb mitochondrial physiology in all/most WT BMDMs [e.g., inflammasome-independent increases in mROS production (Fig. 1*A* and Fig. S1*C*) or hyperpolarization (Fig. 1*B* and Fig. S1 *C* and *E*)]. In contrast, inflammasome-mediated amplification of mitochondrial damage was observed only in a subset of WT cells [e.g., mROS production (Fig. 1*A* and Fig. S1*F*) or depolarization (Fig. 1*B* and Fig. S1 *B*, *D*, and *E*)], which may reflect inflammasome activation only in those cells (consistent with single-cell analysis of inflammasome activation in other studies) (17). These findings support the model that NLRP3 inflammasome activators engage mitochondrial destabilization via stimulus-specific mechanisms (e.g., increased mROS production by ATP but not nigericin) that converge on generation of some signal associated with mitochondrial damage, leading to inflammasome activation and Caspase-1–dependent escalation of mitochondrial damage. No defect in mitochondrial damage was observed in *Casp11*$^{-/-}$ BMDMs (Fig. S1*G*); thus, we attribute defects in *Casp1*$^{-/-}$*Casp11*$^{-/-}$ BMDMs throughout this study to Caspase-1.

Instigation of Mitochondrial Damage by the AIM2 Inflammasome. These findings led us to hypothesize that inflammasomes other than NLRP3 may trigger Caspase-1–dependent mitochondrial

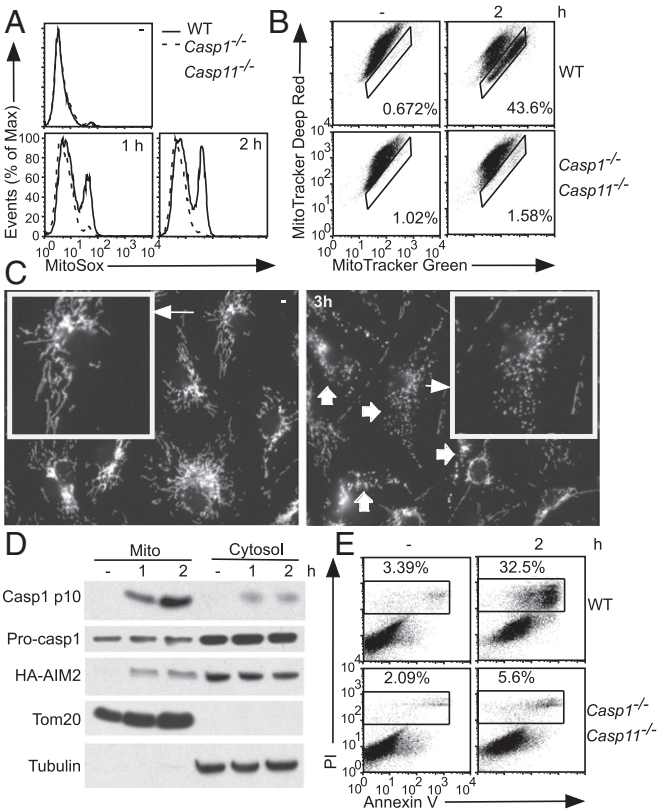

Fig. 2. The AIM2 inflammasome initiates mitochondrial damage. (*A*–*C* and *E*) LPS-primed BMDMs of the indicated genotypes were transfected with DNA. Cells were analyzed by MitoSox (*A*), Mitotracker Green and Deep Red (*B*), or AV/PI (*E*) staining. In *B*, gated cells stain more brightly with Mitotracker Green (i.e., rightward shift), indicating mitochondrial swelling. (*C*) Mitochondrial morphology was examined by immunofluorescence using an antibody to the mitochondria-localized protein Tom20. (*D*) Immortalized macrophage cell lines stably expressing HA-tagged AIM2 were LPS-primed followed by transfection with DNA. Mitochondrial and cytosolic fractions were analyzed by immunoblotting with α-HA and α-Caspase-1 antibodies. Immunoblotting with α-Tom20 and tubulin antibodies served as fractionation controls.

damage. The AIM2 inflammasome is activated by direct binding to cytosolic double-strand DNA and may be a "cleaner" system to determine whether inflammasome activation triggers mitochondrial damage. Indeed activation of the AIM2 inflammasome by DNA transfection led to an increase in mROS production, in a manner dependent on AIM2 and Caspase-1 (Fig. 2*A* and Fig. S2*A*). AIM2 inflammasome activation also led to an increase in Mitotracker Green staining in a subset of WT BMDMs, but not in *Aim2*$^{-/-}$ or *Casp1*$^{-/-}$*Casp11*$^{-/-}$ BMDMs (Fig. 2*B* and Fig. S2*B*), indicating inflammasome-dependent mitochondrial swelling (rather than mitochondrial biogenesis, given the rapid kinetics of the response). Using immunofluorescence microscopy, we showed that the tubular mitochondrial network is fragmented during AIM2 inflammasome activation, in a Caspase-1–dependent manner (Fig. 2*C* and Fig. S2*C*). Inflammasome-mediated mitochondrial damage is also observed in macrophage colony-stimulating factor (MCSF)-generated BMDMs and thioglycollate-elicited peritoneal macrophages (Fig. S2 *D* and *E*). Activated Caspase-1 (p10 subunit) could be localized to the mitochondria after inflammasome activation (Fig. 2*D*), perhaps to allow Caspase-1 to directly cleave mitochondrial proteins and trigger mitochondrial damage (*Discussion*). Thus, AIM2 inflammasome activation leads to Caspase-1–dependent mitochondrial damage as well as induction of pyroptosis (Fig. 2*E*).

During inflammasome activation, only cells with Caspase-1–mediated induction of mitochondrial damage displayed a forward scatter (FSC)/side scatter (SSC) profile consistent with cell death (Fig. S3). Therefore, direct perturbation of the mitochondria by NLRP3 inflammasome activators seems insufficient to induce pyroptosis, which instead correlates with Caspase-1–dependent amplification of mitochondrial damage. Importantly, the kinetics of Caspase-1–mediated mitochondrial damage preceded pyroptosis during AIM2 and NLRP3 inflammasome activation (Fig. S4). Taken together, these findings support a possible contribution of mitochondrial damage to pyroptotic cell death (*Discussion*).

Caspase-1–Mediated Mitochondrial Damage in CAPS. We addressed the relevance of NLRP3 inflammasome-mediated mitochondrial damage in cryopyrin-associated periodic syndrome (CAPS), a spectrum of rare autoinflammatory diseases caused by mutations in *Nlrp3*. Such mutations render the NLRP3 inflammasome aberrantly active in CAPS monocytes and macrophages, presumably because of a reduced threshold for activation (18). Although IL-1β and IL-18 are critical to the pathogenesis of this disease, deficiency of both cytokines in a mouse model of CAPS is not sufficient to abolish inflammation, suggesting the contribution of other Caspase-1–regulated processes (19).

The *Nlrp3*$^{L351P+/-}$*/CreT* mouse line carries a tamoxifen-inducible allele of *Nlrp3* harboring the CAPS mutation L351P (corresponding to human L353P) (18). Consistent with previous studies, LPS stimulation of *Nlrp3*$^{L351P+/-}$*/CreT* BMDMs induces NLRP3 inflammasome-dependent IL-1β production (Fig. S5*A*). LPS stimulation induced mROS production and mitochondrial swelling that is ablated by cotreatment with the Caspase-1 inhibitor VX765 (Fig. 3 *A* and *B*). LPS stimulation of monocytes from CAPS patients also induced mitochondrial swelling and IL-1β production that could be abrogated by VX765 treatment (Fig. 3 *C* and *D*). Finally, VX765 treatment attenuated LPS-mediated pyroptosis in *Nlrp3*$^{L351P+/-}$*/CreT* BMDMs (Fig. 3*E* and Fig. S5*B*). Thus, activation of the NLRP3 inflammasome in CAPS models leads to Caspase-1–dependent mitochondrial damage and pyroptosis, which could contribute to CAPS pathogenesis.

Role of MOMP in Caspase-1–Mediated Mitochondrial Damage. Caspase-8 induces mitochondrial damage through Bid cleavage and consequent induction of MOMP, dissipation of $\Delta\Psi_m$, and mROS production (15); thus, we explored the role of Bid and MOMP in inflammasome-mediated mitochondrial damage and cell death. AIM2 and NLRP3 inflammasome activation triggered release of cytochrome *c* (cyt c) into the cytosol, demonstrating permeabilization of the outer membrane (Fig. 4*A*). At early time points, accumulation of cytochrome *c* in the cytosol paralleled loss from the mitochondria whereas, at late time points, decreased levels of cytosolic cytochrome *c* likely reflected release into culture media as a result of pyroptosis. Inflammasome activation also led to Caspase-1–dependent induction of MPT, as assessed by a calcein-quenching assay in which inner membrane permeabilization enables quenching of matrix calcein by cytoplasmic cobalt (Fig. 4*B* and Fig. S6*A*) (20). Therefore, Caspase-1 triggers mitochondrial permeabilization during inflammasome activation.

Importantly, Bid was cleaved during activation of the AIM2 and NLRP3 inflammasomes, in a largely Caspase-1–dependent manner (Fig. 4*C*). Surprisingly, however, *Bid*$^{-/-}$ BMDMs showed no defect in mROS induction (Fig. 4*D*), mitochondrial swelling (Fig. 4*E*), or MPT (Fig. S6*B*) during AIM2 inflammasome activation. Pyroptotic cell death was likewise normal in *Bid*$^{-/-}$ BMDMs (Fig. S6*C*). Additionally, no defect in mitochondrial damage was observed during NLRP3 inflammasome activation in *Bid*$^{-/-}$ BMDMs (Fig. S6*D*). Induction of MOMP by truncated Bid is dependent on the mitochondrial "gatekeepers" Bax and Bak (15); however, Asc expression is reduced in our *Bak*$^{-/-}$*Bax*$^{\Delta/\Delta}$ immortalized macrophage cell lines, leading to attenuated inflammasome activation (Fig. S6*E*) that would confound analysis of Caspase-1–mediated mitochondrial damage. No defect in inflammasome activation was observed in a recent analysis of Bak$^{-/-}$Bax$^{-/-}$ BMDMs (21), perhaps because Asc expression was not affected (although not reported) and reflecting differences between deletion during macrophage differentiation versus deletion in mature macrophages. Additionally the mROS scavenger MitoTempo was unable to block Caspase-1–mediated mROS induction during AIM2 inflammasome activation (Fig. S6*F*), precluding its use to address the role of mROS induction in pyroptosis. Finally,

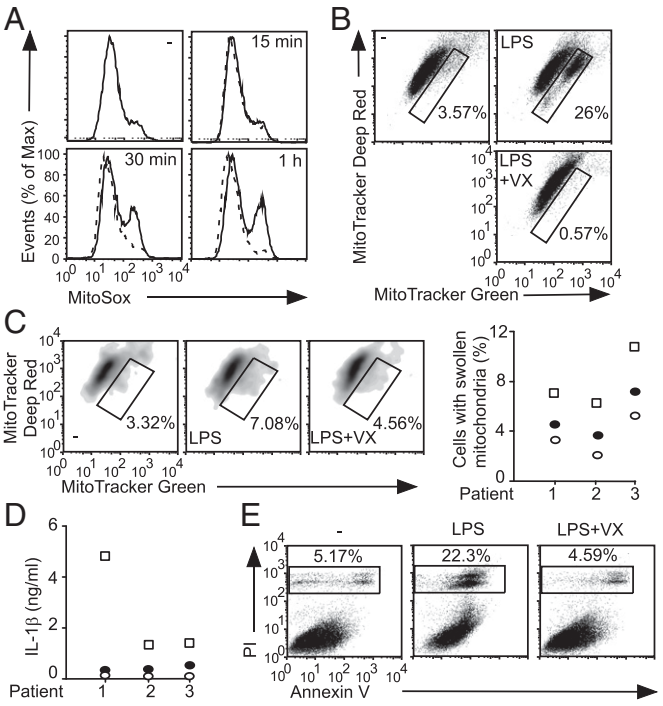

Fig. 3. Caspase-1–dependent mitochondrial damage in CAPS. (*A*, *B*, and *E*) *Nlrp3*$^{L351P+/-}$*/CreT* BMDMs were treated with tamoxifen to permit expression of the mutant *Nlrp3* allele, followed by LPS stimulation ± VX765 (VX). (*A*) MitoSox staining. —, LPS; - - -, LPS plus VX. (*B*) Mitotracker Green and Mitotracker Deep Red staining. Gated cells stain more brightly with Mitotracker Green, indicating mitochondrial swelling. (*C* and *D*) CAPS monocytes were stimulated with LPS ± VX. (*C*) Mitotracker Green and Deep Red staining and (*D*) IL-1β ELISA. In *C*, FACS plots from a representative CAPS patient are shown (*Left*) whereas data from each patient ($n = 3$) are shown as the percentage of monocytes with swollen mitochondria (*Right*). (*E*) AV/PI staining. (*C* and *D*) Open circle, unstimulated; open square, LPS-treated; closed circle, LPS plus VX765 cotreated.

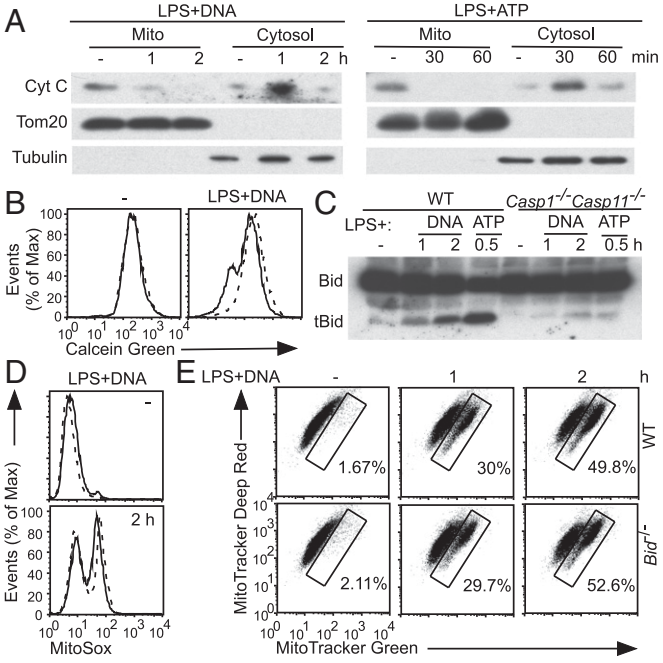

Fig. 4. Inflammasomes engage multiple pathways to trigger mitochondrial damage. (*A–C*) WT and *Casp1*$^{-/-}$*Casp11*$^{-/-}$ BMDMs were stimulated as indicated. (*A*) Immunoblotting of cytosolic and mitochondrial fractions with α-cyt c antibody. (*B*) MPT was assessed by a calcein-quenching assay. —, WT; - - -, *Casp1*$^{-/-}$*Casp11*$^{-/-}$. (*C*) Immunoblotting of whole-cell lysates with α-Bid antibody. *tBid*, truncated Bid. (*D* and *E*) WT and *Bid*$^{-/-}$ BMDMs were treated as indicated followed by (*D*) MitoSox (—, WT; - - -, *Bid*$^{-/-}$) and (*E*) Mitotracker Green and Deep Red staining.

Caspase-3 is activated during inflammasome activation, likely as a consequence of MOMP and cytochrome *c* release, but seems dispensable for amplification of mitochondrial damage (Fig. S6 *G* and *H*). Therefore, inflammasome activation triggers Caspase-1–dependent Bid cleavage and MOMP and MPT induction, but normal mitochondrial damage and pyroptotic cell death in the absence of Bid suggests that Caspase-1 may engage multiple pathways to precipitate mitochondrial disassembly (*Discussion*).

Inflammasomes Mediate Parkin Cleavage and Inhibit Mitophagy. Mitophagy is the process by which damaged mitochondria are targeted for degradation in the autophagy pathway to maintain a pool of healthy mitochondria in the cell (22); thus inflammasome activation may inhibit mitophagy as a means of accumulating dysfunctional mitochondria and amplifying mitochondrial damage. Indeed AIM2 inflammasome activation was associated with a rapid decrease in LC3B lipidation in the mitochondrial fraction relative to untreated cells. Such decrease was ablated in *Casp1*$^{-/-}$*Casp11*$^{-/-}$ BMDMs (Fig. 5*A*), consistent with a Caspase-1–dependent block of mitophagy. Mitochondrial DNA (mtDNA) also accumulated in a Caspase-1–dependent manner during AIM2 inflammasome activation (Fig. 5*B*). The small increase in mtDNA accumulation is expected for the short time course, given ∼2× increases in mtDNA levels in models of prolonged and/or steady-state mitophagy deficiency/impairment (23). Collectively, these findings indicate that inflammasome activation leads to a Caspase-1–dependent block of mitophagy.

To identify the mechanisms by which inflammasomes block mitophagy, we addressed the role of Parkin, a central mitophagy regulator. Parkin is recruited to damaged mitochondria, allowing for ubiquitination of mitochondrial proteins and targeting to the mitophagy pathway (22), and was shown to be cleaved by Caspase-1 (24). Using a 293T cell reconstitution system, we showed that the AIM2 inflammasome cleaves Parkin and that this cleavage required Caspase-1 catalytic activity because it was ablated in cells expressing Caspase-1 C284A (Fig. 5*C*). Parkin cleavage was dependent on D126, which is embedded within a canonical Caspase-1 cleavage site (as predicted by ExPASy PeptideCutter) that is conserved in mouse and human Parkin because the D126A Parkin mutant was not processed by the AIM2 inflammasome (Fig. 5*C*). Importantly, inflammasome activation led to cleavage of ectopically expressed Parkin in immortalized macrophage cell lines, in a manner dependent on Caspase-1 catalytic activity and D126A (Fig. 5*D*). Such Parkin cleavage is predicted to be inactivating based on structure–function analyses and correlations of mutations in this region of the *Parkin* gene with early onset autosomal recessive parkinsonism (25, 26).

Loss of Parkin Enhances Mitochondrial Damage and Pyroptosis. To determine the relevance of mitophagy inhibition and Parkin cleavage during inflammasome activation, we turned to genetic models. In line with a role for Parkin in promoting mitophagy (22), *Parkin*$^{-/-}$ BMDMs displayed increased mitochondrial damage during AIM2 inflammasome activation, with higher mROS production and readily detectable loss of $\Delta\Psi_m$ (Fig. S7*A*), despite comparable Caspase-1 processing (Fig. S7*B*). These effects were small, likely because Parkin cleavage by Caspase-1 in WT cells would phenocopy Parkin deficiency, so we reconstituted a *Parkin*$^{-/-}$ immortalized macrophage cell line with empty vector or cleavage-resistant Parkin-D126A. Cells expressing Parkin-D126A accumulated less mtDNA after inflammasome activation (Fig. 6*A*), consistent with preservation of mitophagic flux. Furthermore, expression of Parkin-D126A attenuated mROS production (Fig. 6*B* and Fig. S7*C*), supporting the idea that Caspase-1–mediated block of mitophagy, critically mediated by Parkin cleavage, amplifies mitochondrial damage. IL-18 production (Fig. 6*C*) and Caspase-1 processing were comparable between the two macrophage cell lines (Fig. S7*D*), indicating that differences in mitochondrial damage were not secondary to varying degrees of AIM2 inflammasome activation.

Cell death was diminished in cells expressing Parkin-D126A (Fig. 6 *D* and *E* and Fig. S7*E*), consistent with the idea that mitochondrial damage can contribute to pyroptosis. Moreover,

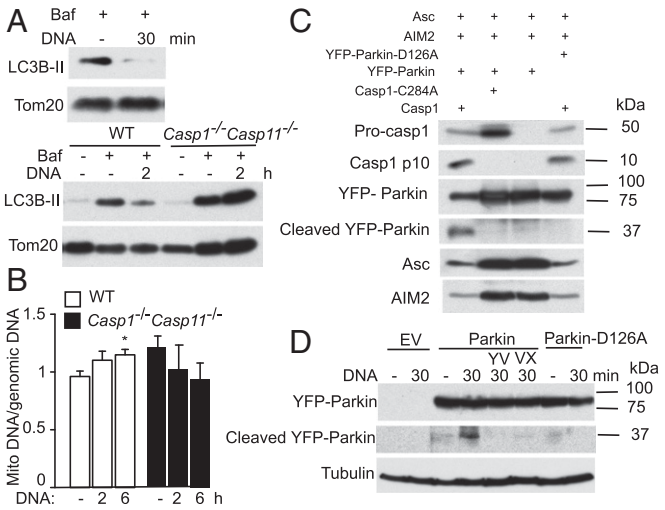

Fig. 5. Inflammasomes inhibit mitophagy and cleave Parkin. (*A* and *B*) WT and *Casp1*$^{-/-}$*Casp11*$^{-/-}$ BMDMs were treated as indicated. (*A*) Immunoblotting of mitochondrial fraction for lipidated LC3 (LC3B-II). The lysosomal inhibitor bafilomycin (Baf) was included to ensure accurate assessment of flux through the mitophagy pathway. (*B*) mtDNA copy number as assessed by qPCR for *cytochrome oxidase I*. *$P < 0.05$ relative to untransfected cells ($n \geq 3$). (*C*) Inflammasomes were reconstituted in 293T cells by transfection of the indicated plasmids. Cleavage of YFP-Parkin (WT or D126A) was examined by immunoblotting with α-Parkin antibody. (*D*) *Parkin*$^{-/-}$-immortalized macrophage cell lines reconstituted with empty vector (EV), YFP-Parkin, or YFP-Parkin-D126A were transfected with DNA ± cotreatment with the Caspase-1 inhibitors YVAD (YV) or VX765 (VX), followed by immunoblotting.

correlating with the differing extent of mitochondrial damage, release of HMGB1 was attenuated in cells expressing Parkin-D126A (Fig. 6*F*). Extracellular histones represent another DAMP that promotes inflammatory responses in sepsis and other inflammatory conditions (27). Histones were released in a Caspase-1–dependent manner during inflammasome activation (Fig. S7*F*), and this response was decreased in the Parkin-D126A macrophage cell line (Fig. 6*F*). Consistently, an increase in pyroptosis (Fig. S7*G*) and DAMP release (Fig. S7*H*) was observed in *Parkin*$^{-/-}$ BMDMs compared with WT BMDMs. Collectively, inflammasome-mediated mitochondrial damage may contribute to pyroptotic cell death and release of DAMPs.

Discussion

Here, we show that mitochondria are a target of activated inflammasomes that can be rapidly dismantled in a Caspase-1–dependent manner. Such mitochondrial damage is manifest as increased mROS production, swelling, dissipation of $\Delta\Psi_m$, loss of outer and inner membrane integrity, and fragmentation of the mitochondrial network. The NLRP3 inflammasome amplifies the initial mitochondrial destabilization (3, 4), leading to disassembly of the organelle, similar to Apaf/Caspase-9 in the apoptosome pathway whereas the AIM2 inflammasome initiates mitochondrial damage, akin to Caspase-8 that is activated by Death Receptors (Fig. S8). Of note, the two inflammasome pathways trigger mitochondrial damage profiles that are similar but not identical (Fig. S9). AIM2 inflammasome activation is associated with robust mROS production and mitochondrial swelling but weak loss of $\Delta\Psi_m$, which is consistent with transient depolarization followed by rebuilding of the proton gradient as has been observed in other settings of apoptosis (20). In contrast, the NLRP3 inflammasome induces mROS production and a prominent loss of $\Delta\Psi_m$. The likely explanation for the differences between the two inflammasome pathways is that, in the context of NLRP3 inflammasome activation, ATP and nigericin directly and immediately perturb mitochondrial physiology, thus affecting the mitochondrial response to Caspase-1 activity. The mitochondrial swelling in LPS-stimulated CAPS monocytes and BMDMs is also consistent with this interpretation. Collectively, these findings show clearly that, during NLRP3 inflammasome activation, early mitochondrial damage is triggered directly by the stimulus, independent of Caspase-1 activity. In some studies of NLPR3 inflammasome activation, discriminating between mitochondrial destabilization triggered by the stimulus or by Caspase-1 in the amplification step may be warranted.

We next sought to elucidate the pathways involved in inflammasome-mediated mitochondrial damage. Although Caspase-1 cleaved Bid during inflammasome activation, this was unexpectedly not critical for MOMP induction, mitochondrial damage, or pyroptosis. The most likely interpretation is that Caspase-1 engages multiple pathways in parallel, including but not limited to Bid processing, that act redundantly to precipitate mitochondrial damage. Execution of cell death by apoptotic caspases is similarly highly redundant, involving inactivation of multiple cellular processes (e.g., mRNA and protein synthesis) and full-scale obliteration of cellular infrastructure (including the cytoskeleton, multiple organelles, and DNA), such that block of any one process is unable to prevent cellular demise (28). In addition to induction of MOMP and MPT, inflammasome activation leads to a rapid block of mitophagy, as indicated by a Caspase-1–dependent accumulation of mtDNA and decrease in mitochondria-associated LC3B lipidation. Such mitophagy block allows for accumulation of dysfunctional mitochondria, amplifies the effects of mitochondrial damage, and is conceptually analogous to caspase-mediated inactivation of prosurvival and homeostatic pathways during apoptosis (28, 29). Interestingly, the inflammasome pathway can promote or inhibit autophagy (7, 8), indicating independent and context-specific regulation of distinct autophagy pathways by inflammasomes. Finally, Caspase-1–mediated cleavage of Parkin, a key mitophagy regulator, contributes to inflammasome-mediated block of mitophagy and mitochondrial damage. In support, mtDNA accumulation and mROS increases after inflammasome activation are attenuated in cells expressing cleavage-resistant Parkin. This is consistent with preservation of mitophagic flux although regulation of other aspects of mitochondrial quality control by Parkin could also contribute (30).

How inflammasomes mediate pyroptotic cell death is an important unresolved question. Supporting a link between mitochondrial damage and pyroptosis, only cells displaying Caspase-1–mediated mitochondrial damage had an FSC/SSC low profile consistent with cell death. Moreover, the kinetics of Caspase-1–mediated mitochondrial damage preceded the appearance of the FSC/SSC low profile. Caspase-1–dependent Parkin cleavage and reduction of mitochondria-associated LC3B lipidation were also detected with rapid kinetics, suggesting that mitophagy inactivation may be an early event after inflammasome activation. Finally, analysis of macrophage cell lines that differ in Parkin expression/activity and the degree of mitochondrial damage indicated that increased mitochondrial damage is associated with enhanced loss of plasma membrane integrity and DAMP release. Collectively, our data suggests that mitochondrial damage could contribute to pyroptotic cell death during inflammasome activation although, at this point, the underlying basis is not clear. High levels of mROS could promote peroxidation of plasma-membrane lipids, thus triggering permeabilization, but the inability to modulate mROS levels with mROS or ROS scavengers precluded a test of this hypothesis. Of note, induction of mitochondrial damage is unlikely to be the only means by which Caspase-1 increases plasma membrane permeability, given the redundancy in the mechanisms of cell death execution during apoptosis and necrosis (28, 31).

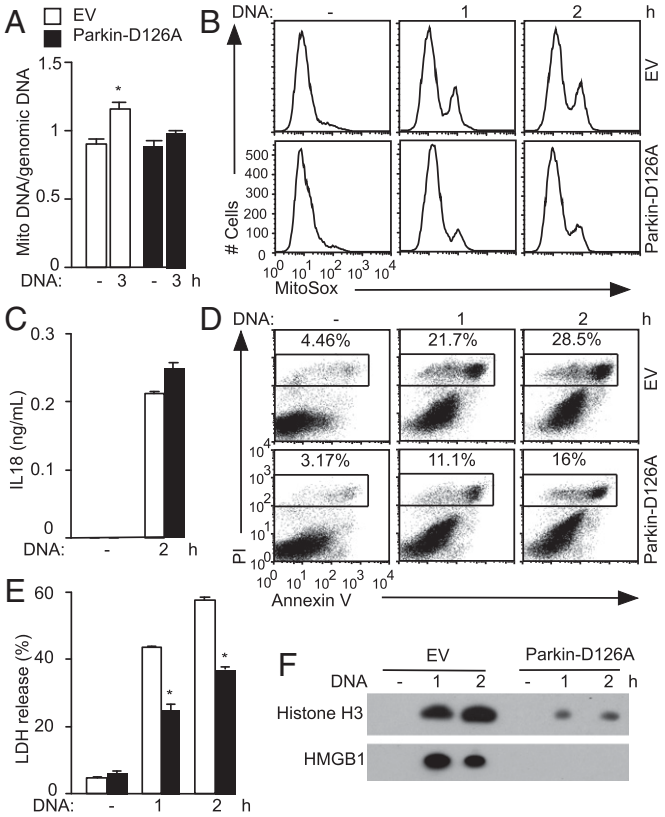

Fig. 6. Parkin expression/activity links mitochondrial damage with pyroptosis. Parkin-deficient immortalized macrophage cell lines reconstituted with empty vector (EV) or YFP-Parkin-D126A were transfected with DNA. (*A*) mtDNA copy number as assessed by qPCR for *cytochrome oxidase I*. (*B*) MitoSox staining and (*C*) IL-18 ELISA. (*D*) AV/PI staining and (*E*) LDH release. (*F*) HMGB1 and histone release were analyzed by immunoblotting of cell-free culture supernatants. (*A*) *$P < 0.05$ relative to untransfected cells. (*E*) $P < 0.05$ relative to cells expressing EV ($n = 3$).

In summary, we showed that Caspase-1 triggers mitochondrial damage upon its activation by the NLRP3 and AIM2 inflammasomes, which may contribute to pyroptotic cell death, increased plasma-membrane permeability, and the release of DAMPs. Future studies should address the role of mitochondrial damage in pyroptosis in various physiological and pathophysiological settings and explore ways to manipulate mitochondrial damage and/or mitophagy as a means of modulating such cell death and amplification of inflammatory responses.

Materials and Methods

Mice. B6/J mice were from The Jackson Laboratory, and *Nlrp3*$^{-/-}$, *Asc*$^{-/-}$, *Casp1*$^{-/-}$*Casp11*$^{-/-}$, *Casp11*$^{-/-}$, and *Bak*$^{-/-}$*Bax*$^{fl/fl}$ mice were gifts of Vishva Dixit (Genentech, South San Francisco, CA), Ruslan Medzhitov (Yale University, New Haven, CT), Junying Yuan (Harvard Medical School, Boston, MA), and Loren Walensky (Dana–Farber Cancer Center, Boston, MA). *Parkin*$^{-/-}$ mice and littermate controls on a B6 × 129 background were provided by Jie Shen (Harvard Medical School, Boston, MA). All other mice were on the B6 background. Animals were maintained at Harvard Medical School, and all animal experiments were done with approval by, and in accordance with regulatory guidelines and standards set by, the Institutional Animal Care and Use committee of Harvard Medical School.

Macrophages. Bone-marrow cultures were prepared using MCSF-containing supernatant. HA-AIM2 macrophage cell lines were generated by retrovirus-mediated delivery of HA-tagged AIM2 into B6 immortalized macrophage cell lines obtained from Kate Fitzgerald (University of Massachusetts Medical School, Worcester, MA). *Parkin*$^{-/-}$ and *Bak*$^{-/-}$*Bax*$^{fl/fl}$ macrophage cell lines were generated by similar immortalization of primary BMDMs. *Parkin*$^{-/-}$ and *Bak*$^{-/-}$*Bax*$^{fl/fl}$ macrophage cell lines were transduced with retrovirus expressing Parkin-D126A and Cre to generate Parkin-D126A–expressing and *Bak*$^{-/-}$*Bax*$^{\Delta/\Delta}$-immortalized macrophage cell lines, respectively. To activate the AIM2 inflammasome, 0.7×10^6 BMDMs were transfected with 1–2 μg/mL calf thymus DNA (Sigma) using Lipofectamine 2000 ± LPS priming as indicated. For the NLRP3 inflammasome, BMDMs were primed with ultrapure LPS (Invivogen) before stimulation with ATP (5 mM) or nigericin (20 μM). Inhibitors were added after LPS priming and 30 min before inflammasome activation.

Mitochondrial Assays. In the last 15–30 min of their stimulation, BMDMs were incubated with MitoSOX (Invitrogen), TMRM (Life Technologies), or MitoTracker Green and Deep Red (Invitrogen). For analysis of MPT, Calcein AM Green (Life Technologies) and $CoCl_2$ were added to BMDMs 15 min before inflammasome activation. Data were acquired on a FACSCalibur flow cytometer (BD Biosciences) and analyzed with FlowJo (TreeStar). Mitochondrial fractionation from BMDMs was performed using the Mitochondria Isolation Kit (Pierce). For analysis of mitochondrial DNA copy number, DNA was isolated using the DNeasy Blood and Tissue kit (Qiagen), and quantitative PCR (qPCR) was used to measure the copy number of mtDNA encoding *cytochrome c oxidase 1*, which was normalized to the copy number of genomic DNA encoding *caspase-11*.

Immunoblotting, ELISA, LDH Release, and AV/PI Staining. For Western blotting analyses, adherent and floating BMDMs were pooled and lysed in SDS sample buffer whereas cell-free supernatants were collected for analysis of secreted proteins. Tubulin immunoblotting was done in each experiment to confirm equivalent protein loading. Antibodies were obtained from Santa Cruz (Caspase-1, Tom20, Parkin, HA, Cytochrome C), Adipogen (Asc), Cell Signaling (Histone 3, LC3B), and Gene Tex (HMGB1). Cell-free supernatants were analyzed for levels of mouse IL-1β (eBioscience), human IL-1β (R&D), and IL-18 (MBL) by ELISA. The LDH release assay was done using the CytoTox 96 Nonradioactive Cytotoxicity Assay kit (Promega). Adherent and floating BMDMs were pooled and stained with AV and PI (Biolegend) followed by flow-cytometry analysis.

Human Monocytes. Peripheral blood mononuclear cells isolated from CAPS patients and unaffected controls by Ficoll gradient were incubated with LPS (100 ng/mL) for 3 h at 37 °C. In some experiments, VX765 (10 μM, dissolved in DMSO; AdooQ) was added 30 min before LPS stimulation. Human subjects provided written informed consent, before inclusion, under protocols approved by the University of California, San Diego Human Research Protections Program and have been performed in accordance with the 1964 Declaration of Helsinki and its later amendments.

Statistics. Statistics were calculated using Excel or GraphPad Prism 6. Comparisons of two groups were analyzed using a two-tailed *t* test as indicated. *P* values <0.05 were considered significant. Data shown in the manuscript are representative of experiments done at least three times. Error bars indicate SEM.

ACKNOWLEDGMENTS. This work was supported by NIH Grant R01AI102964 (to T.H.). T.M. is the recipient of a Japan Society for the Promotion of Science Fellowship and was supported by the Kato Memorial Bioscience Foundation. H.N. was supported by the Kawasaki Sukenobu Fund. L.B. was supported by NIH National Institute of Allergy and Infectious Diseases (NIAID) T32AI007469 and H.H. was supported by NIH NIAID R01 AI52430.

1. Lamkanfi M, Dixit VM (2012) Inflammasomes and their roles in health and disease. *Annu Rev Cell Dev Biol* 28:137–161.
2. Wen H, Miao EA, Ting JP (2013) Mechanisms of NOD-like receptor-associated inflammasome activation. *Immunity* 39(3):432–441.
3. Sutterwala FS, Haasken S, Cassel SL (2014) Mechanism of NLRP3 inflammasome activation. *Ann N Y Acad Sci* 1319:82–95.
4. Horng T (2014) Calcium signaling and mitochondrial destabilization in the triggering of the NLRP3 inflammasome. *Trends Immunol* 35(6):253–261.
5. Keller M, Rüegg A, Werner S, Beer HD (2008) Active caspase-1 is a regulator of unconventional protein secretion. *Cell* 132(5):818–831.
6. Willingham SB, et al. (2009) NLRP3 (NALP3, Cryopyrin) facilitates in vivo caspase-1 activation, necrosis, and HMGB1 release via inflammasome-dependent and -independent pathways. *J Immunol* 183(3):2008–2015.
7. Shi CS, et al. (2012) Activation of autophagy by inflammatory signals limits IL-1β production by targeting ubiquitinated inflammasomes for destruction. *Nat Immunol* 13(3):255–263.
8. Jabir MS, et al. (2014) Caspase-1 cleavage of the TLR adaptor TRIF inhibits autophagy and β-interferon production during Pseudomonas aeruginosa infection. *Cell Host Microbe* 15(2):214–227.
9. Nakahira K, et al. (2011) Autophagy proteins regulate innate immune responses by inhibiting the release of mitochondrial DNA mediated by the NALP3 inflammasome. *Nat Immunol* 12(3):222–230.
10. Misawa T, et al. (2013) Microtubule-driven spatial arrangement of mitochondria promotes activation of the NLRP3 inflammasome. *Nat Immunol* 14(5):454–460.
11. Shimada K, et al. (2012) Oxidized mitochondrial DNA activates the NLRP3 inflammasome during apoptosis. *Immunity* 36(3):401–414.
12. Lamkanfi M, Dixit VM (2010) Manipulation of host cell death pathways during microbial infections. *Cell Host Microbe* 8(1):44–54.
13. Masters SL, et al. (2012) NLRP1 inflammasome activation induces pyroptosis of hematopoietic progenitor cells. *Immunity* 37(6):1009–1023.
14. Doitsh G, et al. (2014) Cell death by pyroptosis drives CD4 T-cell depletion in HIV-1 infection. *Nature* 505(7484):509–514.
15. Tait SW, Green DR (2010) Mitochondria and cell death: Outer membrane permeabilization and beyond. *Nat Rev Mol Cell Biol* 11(9):621–632.
16. Green DR, Kroemer G (2004) The pathophysiology of mitochondrial cell death. *Science* 305(5684):626–629.
17. Murakami T, et al. (2012) Critical role for calcium mobilization in activation of the NLRP3 inflammasome. *Proc Natl Acad Sci USA* 109(28):11282–11287.
18. Brydges SD, et al. (2009) Inflammasome-mediated disease animal models reveal roles for innate but not adaptive immunity. *Immunity* 30(6):875–887.
19. Brydges SD, et al. (2013) Divergence of IL-1, IL-18, and cell death in NLRP3 inflammasomopathies. *J Clin Invest* 123(11):4695–4705.
20. Poncet D, Boya P, Métivier D, Zamzami N, Kroemer G (2003) Cytofluorometric quantitation of apoptosis-driven inner mitochondrial membrane permeabilization. *Apoptosis* 8(5):521–530.
21. Allam R, et al. (2014) Mitochondrial apoptosis is dispensable for NLRP3 inflammasome activation but non-apoptotic caspase-8 is required for inflammasome priming. *EMBO Rep* 15(9):982–990.
22. Youle RJ, Narendra DP (2011) Mechanisms of mitophagy. *Nat Rev Mol Cell Biol* 12(1):9–14.
23. Feng YM, et al. (2013) Decreased mitochondrial DNA copy number in the hippocampus and peripheral blood during opiate addiction is mediated by autophagy and can be salvaged by melatonin. *Autophagy* 9(9):1395–1406.
24. Kahns S, et al. (2003) Caspase-1 and caspase-8 cleave and inactivate cellular parkin. *J Biol Chem* 278(26):23376–23380.
25. Sarraf SA, et al. (2013) Landscape of the PARKIN-dependent ubiquitylome in response to mitochondrial depolarization. *Nature* 496(7445):372–376.
26. Periquet M, et al.; French Parkinson's Disease Genetics Study Group. The European Consortium on Genetic Susceptibility in Parkinson's Disease (2001) Origin of the mutations in the parkin gene in Europe: Exon rearrangements are independent recurrent events, whereas point mutations may result from Founder effects. *Am J Hum Genet* 68(3):617–626.
27. Xu J, et al. (2009) Extracellular histones are major mediators of death in sepsis. *Nat Med* 15(11):1318–1321.
28. Taylor RC, Cullen SP, Martin SJ (2008) Apoptosis: Controlled demolition at the cellular level. *Nat Rev Mol Cell Biol* 9(3):231–241.
29. Norman JM, Cohen GM, Bampton ET (2010) The in vitro cleavage of the hAtg proteins by cell death proteases. *Autophagy* 6(8):1042–1056.
30. Scarffe LA, Stevens DA, Dawson VL, Dawson TM (2014) Parkin and PINK1: Much more than mitophagy. *Trends Neurosci* 37(6):315–324.
31. Liu X, Van Vleet T, Schnellmann RG (2004) The role of calpain in oncotic cell death. *Annu Rev Pharmacol Toxicol* 44:349–370.